Polystyrene foam as a source and sink of chemicals in the marine environment: An XRF study

Turner, Andrew

Published in:
Chemosphere

DOI:
10.1016/j.chemosphere.2020.128087

Publication date:
2021

Polystyrene foam as a source and sink of chemicals in the marine environment: An XRF study

Andrew Turner

School of Geography, Earth and Environmental Sciences, University of Plymouth, Plymouth PL4 8AA, UK

aturner@plymouth.ac.uk

Accepted 19th August 2020

https://doi.org/10.1016/j.chemosphere.2020.128087

Abstract

Polystyrene foam (expanded and extruded polystyrene: EPS and XPS, respectively) is a ubiquitous and pervasive type of marine plastic litter whose physical properties, transport and fate are distinctly different to those of other common (unfoamed) types of thermoplastic litter. In this study, a range of fragments of EPS and XPS retrieved from three beaches in southwest England have been characterised by energy-dispersive X-ray fluorescence spectrometry in order to examine the chemical makeup and potential biological and geochemical impacts and interactions of this type of plastic waste. Analyses performed through sample faces and, in some cases and after dissection, through the material core, revealed variable concentrations of Fe, Ti and Zn among the fragments and, in some cases, within the same sample. This likely reflects the presence of reaction residues and pigments arising from the manufacture of polystyrene, and, for Fe and Ti, significant and heterogeneous ion and mineral acquisition from the environment during transport in suspension or while beached. Acquired oxides of Fe are partly responsible for the chemical fouling observed on the face of most samples and are also able to act as an adsorbent for other metals, like Pb. Detection of Br in many fragments up to concentrations of 11,500 mg kg^{-1} likely results from the incorporation of the flame retardant, hexabromocyclododecane, in EPS and XPS designed for (but not necessarily limited to) the construction sector. These observations suggest that EPS and XPS can act as both a source and sink for contaminants in the marine environment that merit further investigation.

Keywords: polystyrene foam; expanded; extruded; XRF; flame retardants; additives

1. Introduction

Because of its low weight, high strength and excellent thermal-noise insulation and shock-absorbing properties, foamed polystyrene, encompassing expanded polystyrene (EPS) and extruded polystyrene (XPS), is widely used across a range of sectors (e.g., construction, transportation, consumer, maritime) (Wünsch, 2000; Block et al., 2017). However, many of the characteristics that make foamed polystyrene such a popular and useful commodity also ensure that it is a significant and pervasive constituent of the waste stream (Nie et al., 2015; Black et al., 2019).

In the marine environment, EPS and XPS are among of the most abundant forms of plastic litter (Hinojosa and Thiel, 2009; Davis and Murphy, 2015; Che et al., 2018; Chitaka and von Blottnitz, 2018). Sources of polystyrene foam include municipal waste, littering and loss or deterioration of polystyrene-based structures at sea (such as pontoons, floating docks, buoys and boat stands; Hansen et al., 2015; Jang et al., 2020). Unlike other common (unfoamed) thermoplastics, however, a density an order of magnitude lower than that of seawater, coupled with a closed cell structure, results in EPS and XPS waste readily fragmenting in situ and being transported on the ocean surface. Thus, at sea polystyrene foam is subject to considerable windage (Chubarenko et al., 2016), persistent exposure to chemicals resident in the sea surface microlayer (Wurl and Obbard, 2004) and colonisation by rafting organisms (Carson et al., 2013), and when beached material is widely dispersed, abraded, micronised and buried by the action of the wind (Song et al., 2017).

Despite its distinctive physical and mechanical properties, pathways and environmental and biotic interactions, however, foamed polystyrene is generally considered or quantified within the more general pool of marine plastic litter in the scientific literature (Fok et al., 2017; Nabizadeh et al., 2019; Tata et al., 2020). Significant from a geochemical and biological-toxicological perspective and that has yet to be documented is its (non-polymeric) chemical composition, including the presence of any additives and residues arising from manufacture and chemicals acquired from the environment during suspension or beaching. Accordingly, the current study reports on an energy-dispersive X-ray fluorescence (XRF) analysis of EPS and XPS fragments retrieved from various Atlantic- and English Channel-facing beaches of southwest England. XRF spectrometry affords a rapid, non-destructive means of quantifying a range of elements in solids and through a complex series of mathematical algorithms solved iteratively is suited for the analysis of materials of low-density like plastics and including foams (Piorek, 2004; Furl et al., 2012). XRF is also able to provide information on the spatial distribution of elements, including the relative significance of those incorporated into the matrix and held at the surface.

2. Methods

2.1. Sample collection

As part of a number of research programmes studies aimed at examining marine litter more generally (Turner and Solman, 2016) or targeting samples for experimental studies (Turner and Lau, 2016), samples of EPS and XPS had been retrieved manually during late spring or early autumn of 2015 from three beaches in southwest England. Namely, Tregantle (50.353, -4.271), a large, southwest-facing sandy beach on the south coast of Cornwall that is backed by high cliffs, Constantine Bay (50.539, -5.027), a large, southwest-facing sandy beach on the north coast of Cornwall that is backed by a dune system, and Mount Batten (50.356, -4.127), a small, sand-gravel beach in the partly-urbanised embayment of Plymouth Sound. Polystyrene fragments were usually abundant on the latest (or highest) strandline and on the back-beach near to the cliff or dune base. In the laboratory, any loosely adherent material was dislodged or brushed off under tap water before samples were dried under desiccation at room temperature for 96 h. Samples were then weighed and photographed and stored in individual polyethylene specimen bags in the dark until required for analysis.

2.2. XRF analysis

Samples were analysed by energy-dispersive portable XRF spectrometry using a Niton XL3t 950 He GOLDD+ configured in a laboratory accessory stand. The instrument was operated in a customised, standardless 'plastics' mode and because of the low density of foamed polystyrene, a thickness correction algorithm was always applied after measuring the thickness of material through the measurement surface using Allendale digital callipers (Turner and Solman, 2016). Samples were counted for periods ranging from 60 to 180 s, depending on material thickness, that were distributed in a 2:1 ratio between a low energy range (20 kV and 100 μA) and main energy range (50 kV and 40 μA). Spectra were quantified by fundamental parameter coefficients to yield concentrations on a dry weight basis (in mg kg^{-1}) and with a counting error of 2σ (95% confidence). Up to 18 elements may be analysed in the plastics mode but the focus of the present study was on those that are known to be used in various plastics (Ba, Br, Fe, Sb, Ti, Zn), act as proxies for hydrogenous and detrital phases (Fe, Ti) or are contaminants of toxicological concern (Br, Cd, Pb).

By default, the measurement face was an 8-mm diameter circular area of the central region of the largest or flattest face. For selected samples larger than about 3 cm in diameter, between four and eight measurements were made at different locations over the face to examine the distribution of elements within the matrix. Here, the small-spot facility of the instrument was employed in order to

focus the X-ray beam into a 3-mm diameter circular area. For these samples, were possible, material was sliced through the thickest axis with a stainless steel scalpel and the central core analysed.

As a performance check, polyethylene reference discs Niton PN 180-619 (Ba = 688 $\pm$ 45 mg kg^{-1}; Cd = 150 $\pm$ 6 mg kg^{-1}; Pb = 150 $\pm$ 12 mg kg^{-1}; Sb = 96 $\pm$ 10 mg kg^{-1}) and Niton PN 180-554 (Br = 495 $\pm$ 20 mg kg^{-1}; Cd = 292 $\pm$ 20 mg kg^{-1}; Pb = 1002 $\pm$ 40 mg kg^{-1}) were analysed throughout each measurement session, with the instrument returning concentrations that were consistently within 10% of certified values. Detection limits varied depending on counting time, sample thickness and whether the small-spot was engaged but indicative values based on the lowest counting errors returned throughout the study ranged from about 10 mg kg^{-1} for Br, Pb and Ti to 100 mg kg^{-1} for Ba and Sb in EPS and about 20 mg kg^{-1} for Br, Pb and Ti to 250 mg kg^{-1} for Ba and Sb in XPS. Analytical precision, defined by repeat measurements (n = 5) of the same area of sample, was generally better than 10% but could be as high as 25% if concentrations were close to the detection limit and determined with the small-spot facility.

2.3. Polystyrene confirmatory analysis

For sixteen samples that were particularly weathered or discoloured, confirmation of the polymeric matrix was achieved by attenuated total reflectance Fourier Transform Infrared (FTIR) spectrometry using a Bruker Vertex 70. Here, 1-3 mm offcuts of the sample surface were clamped against the ATR diamond crystal and spectra were recorded with 16 scans in the region 4000 to 600 cm^{-1} and at a resolution of 4 cm^{-1}. After being smoothed, baseline-corrected and normalised via Bruker OPUS 7 software, spectra were matched up with spectra of polystyrene contained in various reference libraries.

3. Results

A total of 86 samples, exemplified in Figure 1, were returned to the laboratory for characterisation. Samples ranged in size from individual foamed beads of about 4 mm in diameter and 30 mg in mass to fragments of about 10 cm in length and weighing up to 10 g. EPS samples (n = 67) were identified from presence of the distinctive beaded (cellular) structure while XPS samples (n = 19) were usually unstructured, flatter and smoother. Where material was heavily fouled or discoloured, FTIR analysis confirmed the polymeric composition of both EPS and XPS from aromatic ring stretches at 1600 cm^{-1} 1490 cm^{-1} and aromatic CH out-of-plane bends at 694 cm^{-1} and 537 cm^{-1} (Noda et al., 2007).

Most samples of EPS were well-rounded, unidentified fragments that contained surficial cracks or pits, and the polystyrene itself was usually white or off-white. Dissection of samples revealed a "clean" interior that was generally free of fouling or particle intrusion (Figure 1h). Samples of XPS tended to be thinner and more ragged (Figures 1c and 1e), and displayed a broader range of colours that that included white, beige, blue or green. Some samples of XPS had evidently been derived from single-use food or drink containers that likely had a local (littering) origin. With the exception of the latter type of sample, most foamed fragments were visibly discoloured at the face (and relative to the core) by orange-brown chemical fouling, with some EPS soiled by fine particulates trapped in the pore space between weathered beads or stained by oil.

Summary statistics for the concentrations of the elements in the samples as determined by XRF are shown in Table 1, with the full dataset shown in Appendix A. Data in Table 1 are pooled for the three locations and a direct comparison is made between the two different types of foamed polystyrene. Note that measurements were made in the central region of the largest face and, because of the low density of the material, values reported signify concentrations that are representative of the entire depth of sample rather than the measurement face. Note also that elemental detection limits for XPS were about double the corresponding detection limits for EPS because of the lower thickness of the former samples. Among the elements considered, Fe and Ti were most commonly detected and exhibited the highest mean, median and maximum concentrations. Bromine and Zn were detected in about 60 cases each, Pb was detected in 14 samples of EPS and Ba was detected in eight samples of EPS; Sb was detected in just one sample of XPS and Cd was never detected (< 25 mg kg^{-1}). A series of Kruskal-Wallis tests performed in Minitab *v*19 revealed that median concentrations of Fe and Ti in EPS were significantly greater than respective median concentrations in XPS ($H > 15$, $p < 0.01$) but there was no significant difference in median concentrations of either Br or Zn between the material types ($H < 1$, $p > 0.1$).

Table 1: Detection frequency for the different elements and summary statistics for their concentrations (in mg kg^{-1}).

	Ba	Br	Cd	Fe	Pb	Sb	Ti	Zn
EPS (n = 19)								
detection, %	9.0	79.1	0	100	20.9	0	98.5	65.7
mean	536	1610		9620	50		2670	392
median	438	224		8170	20		1620	173
min	350	12		282	11		68	42
max	1060	11500		29100	175		50900	3560
XPS (n = 19)								
detection, %	0	31.6	0	89.5	0	5.3	94.7	89.5
mean		890		2300		373	579	193
median		120		1150			518	135
min		27		85			25	36
max		4710		7120			1740	674

Figure 2 shows the spatial distribution of Br, Fe, Ti and Zn in five samples of EPS (samples of XPS were generally too thin to perform this characterisation (see Figure 1) and Pb was never detected in the core of EPS). Specifically, the variation in concentrations measured on the largest or flattest face, $[]_{face}$, are shown against single or replicate measurements of concentration of the core, $[]_{core}$, once the sample had been dissected. For Br, relative standard deviations (rsds) of concentrations are < 30% except for the face of one sample (rsd ~ 65%). Overall, however, mean concentrations lie close to unit slope, indicating that concentrations determined through the face and in the core are similar. The distributions of Fe and Ti are are rather scattered on the charts, and especially in the *y*-axis where rsds of up to 50% are observed, and concentrations of both elements measured on the face are similar to (n = 2), greater than (n = 2) or lower than (n = 1) corresponding concentrations measured in the core. Regarding Zn, with the exception of one sample lying well above unit slope, concentrations measured on the face and core are similar and exhibit relatively little variation among replicate measurements. Note that Ba, not plotted, was detected on the face and core of one sample and returned concentrations that were similar (676 $\pm$ 47 mg kg^{-1} and 672 $\pm$ 25mg kg^{-1}, respectively).

4. Discussion

The results of this study are consistent with the reaction residues and functional additives known to be present in foamed polystyrene or in thermoplastics more generally but are significant in providing an insight into the concentration ranges of these chemicals in EPS and XPS fragments encountered in the marine environment. Thus, the detection of Fe in most samples may be attributed to the use of Fe_2O_3 as a catalyst in the production of styrene (Wünsch, 2000) while the presence of Zn in many cases, and at least in EPS, may be attributed to residual Zn stearate that is often used to ensure

uniform cell nucleation in the production of the expanded material (European Union, 2008). The detection of Ti in most cases reflects the common usage of TiO_2, and principally rutile, as a pigment that is blended or moulded into the material to provide a high refractive index and chemical stability (Murphy, 2001), while the lack of Ba is due to the avoidance of fillers of high specific gravity, like $BaSO_4$, in products specifically designed to be lightweight (Turner and Filella, 2020).

Detectable Br in a high proportion of EPS samples and about a third of XPS samples is attributed to the presence of brominated flame retardants (Gallen et al., 2014). XRF is unable to discriminate different brominated compounds but the most commonly used in foamed PS, and in particular that destined for the construction sector, was 1,2,5,6,9,10-hexabromocyclododecane (HBCD). Production of HBCD began in the 1980s until it was added to Annex A of persistent organic pollutants in the Stockholm Convention that require elimination (United Nations, 2013) and effectively banned (Schlummer et al., 2017). HBCD was added to foamed polystyrene at concentrations that are low relative to concentrations of other halogenated compounds used to flame-retard plastics (about 0.7 to 2.5% by weight; Alaee et al., 2003). Moreover, and unlike flame-retarded plastics more generally, foamed PS impregnated with HBCD did not require the addition of antimony trioxide (Sb_2O_3) as a synergist to meet various building code specifications (Papazoglou, 2004), thereby accounting for the lack of detection of Sb in the current samples (Table 1).

Assuming that Br concentrations result from only HBCD and given that the fractional mass contribution of Br to HBCD is 0.75, the maximum concentration of the flame retardant reported in Table 1 is about 15,300 mg kg^{-1} (or 1.5% of HBCD by weight). This value is in good agreement with the maximum concentration of HBCD measured directly in EPS and XPS fragments retrieved from the north Pacific Ocean (Jang et al., 2017) and is within the content range required for flame-retardancy of construction material (Alaee et al., 2003). This observation, coupled with Br being undetected in samples of XPS that were evidently related to single-use food-drink containment (such as take-out trays and Styrofoam cups) suggests that the majority of samples collected herein originate from the construction industry. However, this may not necessarily be the case because a single grade of HBCD often appears to have been used for wider production (for use in both construction and packaging, for example) (Lassen et al., 2019) and there is evidence for the uncontrolled use or recycling of the flame retardant (Rani et al., 2014; Abdullah et al., 2018). The latter pathway would account for the high variability of Br concentrations among the samples and the occurrence of concentrations well below those required for flame-retardancy in many cases.

From a regulatory perspective, the EU has recently introduced a low concentration limit of 0.1% (1000 mg kg^{-1}) by weight for certain brominated compounds, including HBCD, above which items

may not be recycled, and a limit of 0.01% (100 mg kg^{-1}) above which products are not permitted for sale in the EU (European Commission, 2016). Converting the Br measurements summarised in Table 1 into HBCD concentrations reveals that 18 samples of EPS and one sample of XPS would be non-compliant for recycling and that 43 samples of EPS and three samples of XPS would be non-compliant for resale.

Another factor to consider that has a potentially significant impact on elemental concentrations measured in the EPS and XPS samples is the acquisition of chemicals from or their loss to the environment while at sea or once beached. Since the additives and residues identified above are not covalently bonded to the polymeric matrix, there is scope for migration from foamed polystyrene into seawater. Predicted or measured diffusion rates for ions and compounds in virgin plastics vary considerably but are generally very small (Town et al., 2018), with estimates of diffusion half-lives for various brominated flame retardants on the order of tens of thousands of year or more (Sun et al., 2019). That said, physical and chemical processes acting on plastics in the marine environment, including digestion by animals, may considerably accelerate leaching (Tanaka et al., 2015; Smith and Turner, 2020) and result in a more heterogeneous distribution of chemicals in the weathered matrix (Turner et al., 2020).

With a specific surface area of about 2 $m^2 g^{-1}$ and a point of zero charge of about 4.7, the inherent surface properties of foamed polystyrene are more favourable for the adsorption of metal ions than many other polymers (Zhang et al., 2018). Moreover, the low density of EPS and XPS ensures that material is exposed to elevated concentrations of metals and other contaminants in the sea surface microlayer (Wurl and Obbard, 2004). On aging, the surfaces of EPS and XPS become discoloured and fouled by organic and inorganic precipitates, a process that is visibly and chemically heterogeneous (see Figure 1 and the *y*-axis distributions of Fe and Ti in Figure 2) and that likely further enhances the adsorption of contaminant metals like Pb. In theory, the degree of metal enrichment at the face may be related to the age of sample or the time spent in suspension in seawater. However, it is important to bear in mind that metal enrichment at or near the polymer surface may also arise from the entrapment of fine detrital particulates within the surficial interstices of the material that evade removal during sample cleaning. Moreover, because of the low density of foamed polystyrene, measurements undertaken through the face are, strictly, more representative of concentrations through the entire sample (and not the measurement face alone).

Amongst the elements analysed, there was a strong association between Fe and Ti once two samples with exceptionally high Ti concentrations (> 10,000 mg kg^{-1}) had been excluded (Figure 3a). Results of regression analyses of all data and individual data sets defining the faces of XPS and EPS

247 samples and the central core of EPS samples are shown in Table 2. Thus, concentrations of Fe and Ti
248 are significantly related in each case, with relatively small intercepts (*c*) and slopes (*m*) that range
249 from 3.90 for XPS faces to 6.72 for EPS cores. A value of *m* that is greater in EPS than XPS suggests
250 that residual, catalytic Fe relative to pigmented Ti is higher in EPS, while the greatest value of *m* that
251 defines the cores of EPS suggests that the ratio of authigenic Fe to Ti acquired from the environment
252 is lower than the elemental ratio arising from manufacture.

253 In contrast, a lack of association was observed between the concentrations of Fe and Br (Figure 3b).
254 Here, concentrations of HBCD and residual Fe appear to be unrelated during the manufacturing
255 process, perhaps because of the uncontrolled use and recycling of the former (Rani et al., 2014).
256 Moreover, while Fe is readily acquired from the environment, HBCD and other forms of Br are not
257 taken up appreciably and may be more subject to heterogeneous leaching from the matrix (Tanaka
258 et al., 2015).

259

260 Table 2: Statistical parameters defining relationships between concentrations of Fe and Ti shown in
261 Figure 3a.

	n	*m*	*c*	r^2	*p*
all data*	85	5.85	370	0.674	<0.0001
XPS	16	3.90	298	0.752	<0.0001
EPS	64	5.53	1140	0.576	<0.0001
EPS-core	5	6.72	-412	0.989	0.0005

262

263 *After exclusion of two samples where [Ti] > 10,000 mg kg^{-1}.

264

265 **5. Conclusions**

266 The findings of this study reveal that waste EPS and XPS can act as both a source and sink of
267 contaminants in the marine environment. Reaction residues and additives in the matrix detected by
268 XRF include Fe_2O_3, TiO_2 and brominated compounds (presumably dominated by the flame retardant,
269 HBCD), with the latter of greatest environmental concern. Accumulations of Fe- and Ti-based ions
270 and minerals on the surface of polystyrene foam reflect the propensity of the material to acquire
271 chemicals from the environment, with evidence that these phases can also act as adsorbents of
272 more harmful metals like Pb. Given the ability of EPS and XPS to undergo long-range transport and
273 ready fragmentation, it is recommended that future research focuses on the geochemical reactivity
274 and biological interactions of this type of plastic litter.

Acknowledgements

This study was funded by a HEIF Plymouth Marine Institute Grant.

Appendix A: Supplementary material

Supplementary data to this article can be found online at…

References

Abdullah, M.A.E., Sharkey, M., Berresheim, H., Harrad, S., 2018. Hexabromocyclododecane in polystyrene packaging: A downside of recycling? Chemosphere 199, 612-616.

Alaee, M., Arias, P., Sjodin, A., Bergman, A., 2003. An overview of commercially used brominated flame retardants, their applications, their use patterns in different countries/regions and possible modes of release. Environment International 29, 683–689.

Black, J.E., Kopke, K., O'Mahony, C., 2019. Towards a circular economy: using stakeholder subjectivity to identify priorities, consensus, and conflict in the Irish EPS/XPS market. Sustainability 11, 6834 doi:10.3390/su11236834

Block, C., Brands, B., Gude, T., 2017. Packaging Materials 2. Polystyrene for Food Packaging Applications. ILSI Europe, Brussels, 36pp.

Carson, H.S., Nerheim, M.S. Carroll, K.A., Eriksen, M., 2013. The plastic-associated microorganisms of the North Pacific Gyre. Marine Pollution Bulletin 75, 126-132.

Che, C.L., Kuo, P.H., Lee, T., Liu, C.H., 2018. Snow lines on shorelines: Solving Styrofoam buoy marine debris from oyster culture in Taiwan. Ocean and Coastal Management 165, 346-355.

Chitaka, T.Y., von Blottnitz, H., 2019. Accumulation and characteristics of plastic debris along five beaches in Cape Town. Marine Pollution Bulletin 138, 451-457.

Chubarenko, I., Bagaev, A., Zobkov, M., Esiukova, E., 2016. On some physical and dynamical properties of microplastic particles in marine environment. Marine Pollution Bulletin 108, 105-112.

Davis, W, Murphy, A.G., 2015. Plastic in surface waters of the Inside Passage and beaches of the Salish Sea in Washington State. Marine Pollution Bulletin 97, 169-177.

European Commission, 2016. Regulation (EC) No 850/2004 of the European Parliament and of the Council of 29 April 2004 on Persistent Organic Pollutants and Amending Directive 79/117/EEC. https://eur-lex.europa.eu/legal-content/EN/TXT/?uri=CELEX:02004R0850-20160930 accessed 6/20.

European Union, 2008. Risk Assessment: Zinc distearate. EUR 21168 EN, Luxembourg, 188pp.

Fok, L., Cheung, P.K., Tang, G.D., Li, W.C., 2017. Size distribution of stranded small plastic debris on the coast of Guangdong, South China. Environmental Pollution 220, 407-412.

Furl, C., Mathieu, C., Roberts, T., 2012. Evaluation of XRF as a screening tool for metals and PBDEs in children's products and consumer goods. Environmental Assessment Program Report No. 12-03-009, Washington State Department of Ecology, Olympia, WA, 69pp.

Gallen, C., Banks, A., Brandsma, S., Baduel, C., Thai, P., Eaglesham, G., Heffernan, A., Leonards, P., Bainton, P., Mueller, J.F., 2014. Towards development of a rapid and effective non-destructive testing strategy to identify brominated flame retardants in the plastics of consumer products. Science of the Total Environment 491/492, 255-265.

Hansen, A.A., Rodbotten, M., Lea, P., Rotabakk, B.T., Birkeland, S., Pettersen, M.K., 2015. Effect of transport packaging and repackaging into modified atmosphere on shelf life and quality of thawed Atlantic cod loins. Packaging Technology and Science 28, 925-938.

Hinojosa, I.A., Thiel, M., 2009. Floating marine debris in fjords, gulfs and channels of southern Chile. Marine Pollution Bulletin 58, 341-350.

Jang, M., Shim, W.J., Han, G.M., Rani, M., Song, Y.K., Hong, S.H., 2017. Widespread detection of a brominated flame retardant, hexabromocyclododecane, in expanded polystyrene marine debris and microplastics from South Korea and the Asia-Pacific coastal region. Environmental Pollution 231, 785-794.

Jang, M., Shim, W.J., Cho, Y., Han, G.M., Song, Y.K., Hong, S.H., 2020. A close relationship between microplastic contamination and coastal area use pattern. Water Research 171, 115400 DOI: 10.1016/j.watres.2019.115400

Lassen, C., Warming, M., Kjøholt, J., Jakobsen, L.G., Vrubliauskiene, N., Norichkov, B., Strand, J., Feld, L., Bach, L., 2019. Survey of Polystyrene Foam (EPS and XPS) in the Baltic Sea. Danish Fisheries Agency/Ministry of Environment and Food of Denmark, 166pp.

Murphy, J., 2001. Additives for Plastics Handbook, second edition. Elsevier Science, Oxford, 471pp.

Nabizadeh, R., Sajadi, M., Rastkari, N., Yaghmaelan, K., 2019. Microplastic pollution on the Persian Gulf shoreline: A case study of Bandar Abbas city, Hormozgan Province, Iran. Marine Pollution Bulletin 145, 536-546.

Nie, Z.Q., Yang, Z.L., Fang, Y.F., Tang, Z.W., Wang, X.R., Die, Q.Q., Gao, X.B., Zhang, F.S., Wang, Q., Huang, Q.F., 2015. Environmental risks of HBCDD from construction and demolition waste: A contemporary and future issue. Environmental Science and Pollution Research 22, 17249-17252.

Noda I., Dowrey A.E., Haynes J.L., Marcott C., 2007. Group Frequency Assignments for Major Infrared Bands Observed in Common Synthetic Polymers. In: Mark J.E. (eds) Physical Properties of Polymers Handbook. Springer, New York, NY. https://doi.org/10.1007/978-0-387-69002-5_22

Papazoglou, E.S., 2004. Flame retardants for plastics, in: C.A. Harper (ed.), Handbook of Building Materials for Fire Protection, McGraw-Hill, New York, pp4.1-4.88.

Piorek, S., 2004. Feasibility of analysis and screening of plastics for heavy metals with portable x-ray fluorescence analyser with miniature x-ray tube. GPEC 2004 Paper abstract #14.

Rani, M., Shim, W.J., Han, G.M., Jang, M., Song, Y.K., Song, S.H., 2014. Hexabromocyclododecane in polystyrene-based consumer products: an evidence of unregulated use. Chemosphere 110, 111-119.

346 Schlummer, M., Mäurer, A., Wagner, S., Berrang, A., Fell, T., Knappich, F., 2017. Recycling of flame
347 retarded waste polystyrene foams (EPS and XPS) granules free of hexabromocyclododecane (HBCD).
348 Advances in Recycling and Waste Management 2.2 DOI: 10.4172/2475-7675.1000131

349 Smith, E.C., Turner, A., 2020. Mobilisation kinetics of Br, Cd, Cr, Hg, Pb and Sb in microplastics
350 exposed to simulated, dietary-adapted digestive conditions of seabirds. Science of the Total
351 Environment 733, 138802.

352 Song, Y.K., Hong, S.H., Jang, M., Han, G.M., Jung, S.W., Shim, W.J., 2017. Combined effects of UV
353 exposure duration and mechanical abrasion on microplastic fragmentation by polymer type.
354 Environmental Science and Technology 51, 4368-4376.

355 Tanaka, K., Takada, H., Yamashita, R., Mizukawa, K., Fukuwaka, M.A., Watanuki, Y., 2015. Facilitated
356 leaching of additive-derived PBDEs from plastic by seabirds' stomach oil and accumulation in tissues.
357 Environmental Science and Technology 49, 11799-11807.

358 Tata, T., Belabed, B.E., Bououdina, M., Bellucci, S., 2020. Occurrence and characterization of surface
359 sediment microplastics and litter from North African coasts of Mediterranean Sea: Preliminary
360 research and first evidence. Science of the Total Environment 713, 136664.

361 Town, R.M., van Leeuwen, H.P., Blust, R., 2018. Biochemodynamic features of metal ions bound by
362 micro- and nano-plastics in aquatic media. Frontiers in Chemistry
363 https://doi.org/10.3389/fchem.2018.00627

364 Turner, A., Lau, K.S., 2016. Elemental concentrations and bioaccessibilities in beached plastic foam
365 litter, with particular reference to lead in polyurethane. Marine Pollution Bulletin 112, 265-270.

366 Turner, A., Solman, K.R., 2016. Analysis of the elemental composition of marine litter by field-
367 portable-XRF. Talanta 159, 262-271.

368 Turner, A., Filella, M., 2020. The influence of additives on the fate of plastics in the marine
369 environment, exemplified with barium sulphate. Marine Pollution Bulletin 158, 111352.

370 Turner, A., Arnold, R., Williams, T., 2020. Weathering and persistence of plastic in the marine
371 environment: Lessons from LEGO. Environmental Pollution 262, 114299.

372 United Nations, 2013. Stockholm Convention on Persistent Organic Pollutants.
373 C.N.934.2013.TREATIES-XXVII.15 (Amendment to Annex A).
374 https://treaties.un.org/doc/Publication/CN/2013/CN.934.2013-Eng.pdf accessed 6/20.

375 Wurl, O., Obbard, J.P., 2004. A review of pollutants in the sea-surface microlayer (SML): a unique
376 habitat for marine organisms. Marine Pollution Bulletin 48, 1016-1030.

377 Wünsch, J.R., 2000. Polystyrene: Synthesis, Production and Applications. RAPRA report, Shawbury,
378 UK, 160 pp.

379 Zhang, H., Wang, J., Zhou, B., Zhou, Y., Dai, Z., Zhou, Q., Chriestie, P., Luo, Y., 2018. Enhanced
380 adsorption of oxytetracycline to weathered microplastic polystyrene: Kinetics, isotherms and
381 influencing factors. Environmental Pollution 243, 1550-1557.

382

Figure 1: Examples of the EPS (a,b,d,f,g,h) and XPS (c,e) samples retrieved from beaches of southwest England. Annotated bars are approximately 1 cm.

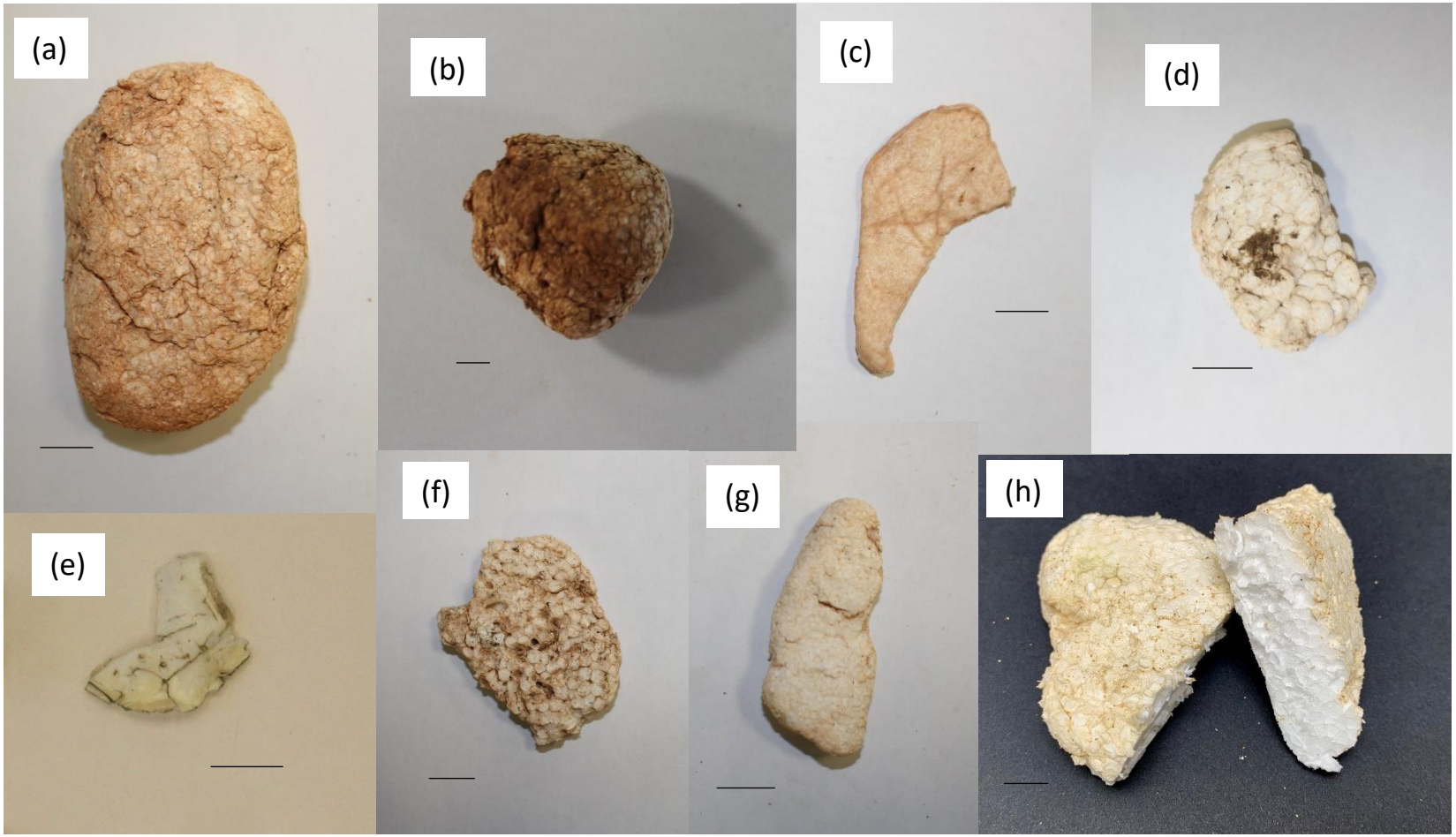

Figure 2: Elemental concentrations measured at various locations on the face versus concentrations measured in the core of five samples of EPS. (a) Br, (b) Fe, (c) Ti, (d) Zn; errors are one standard deviation about the mean (*n* = 3 to 7) and the red line signifies unit slope.

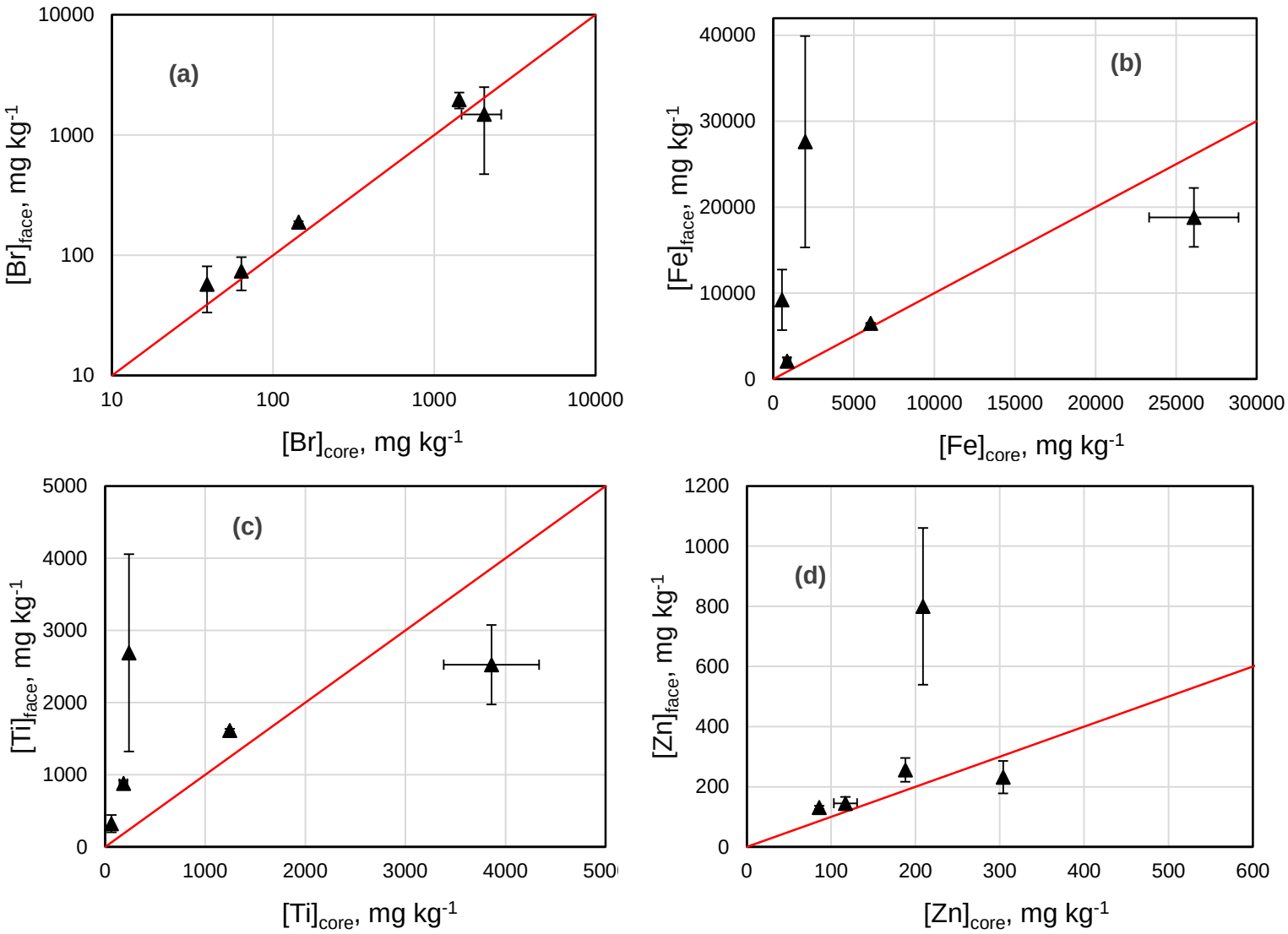
(a)
10000
1000
100
10
10
100
1000
10000
[Br]face, mg kg-1
[Br]core, mg kg-1
(b)
40000
30000
20000
10000
0
0
5000
10000
15000
20000
25000
30000
[Fe]face, mg kg-1
[Fe]core, mg kg-1
(c)
5000
4000
3000
2000
1000
0
0
1000
2000
3000
4000
[Ti]face, mg kg-1
[Ti]core, mg kg-1
(d)
1200
1000
800
600
400
200
0
0
100
200
300
400
500
600
[Zn]face, mg kg-1
[Zn]core, mg kg-1

Figure 3: Concentrations of (a) Fe versus Ti and (b) Fe versus Br measured on the central face of XPS and EPS samples and in the core of selected EPS fragments. Parameters defining Fe versus Ti are shown in Table 2.